STRUCTURAL BEHAVIOR OF HIGH PERFORMANCE LIGHTWEIGHT AGGREGATE CONCRETE BEAMS REINFORCED WITH FIBERS

H. K. Ahmed[1], B.A. Hamid[2]

Abstract

Structural lightweight aggregate concrete solves weight and durability problems in buildings and structures. Recent advances in materials technology have accelerated the development of high performance concrete using lightweight aggregate. The main aim of this investigation is to produce high performance lightweight aggregate concrete beams reinforced with fiber and to study the effect of some variables on structural behavior of the beams such us, type of fiber, volume fraction of fibers and the use of lightweight sand as partial replacement of normal sand

The experimental program included the use of pumice as a coarse lightweight aggregate, super-plasticizer admixture and silica fume to produce high performance lightweight concrete mix. Two types of steel fibers were used also, namely crimped and hooked the fibers content was (0.5, 0.75, 1.25) % by volume. The selected mix was used in casting beams (2000x150x25) mm.

The work was covered investigating the flexural properties of beam specimens such as first crack and ultimate load, moment capacity, ductility and toughness.

The flexural test results for specimen beams showed that the failure load increased for both types of fibers. The results also showed that the cracking load increased in comparison to control beam.The method of analysis of HPLWC beams with fibers is shown to give a very good agreement with experimental data.

Keywords: high performance concrete, lightweight concrete, flexural tests, load deflection curve, ductility, toughness index, fiber reinforced concrete.

1. Introduction

The cost and functionality of any project is a significant issue. Replacing structural normal-weight-aggregate concrete with lightweight-aggregate reduces dead loads by 25-30%. The use of this type of concrete is usually predicated on the reduction of project cost, improved functionality or combination of both. Cost reduction may come from smaller size

[1] Hisham Khalid Ahmed, Dept of Building & Construction Engineering, University of Technology, Baghdad-Iraq, email: hish1950@yahoo.com

[2] Brwa Ahmed Hamid, M. Sc. Structural Engineering, Asia Cell Company, Suleimanyiah–Iraq, email: brwa962@gmail.com

foundation elements and less steel reinforcement. The reduction in dead loads may result in smaller supporting members resulting in a major reduction in cost and at the same time this will mean reduced inertial seismic forces. Improvement in the functionality of rehabilitated bridges through widening the deck or adding additional traffic lane without structural or foundation modification will be possible in addition to using longer and larger precast-prestress elements without increasing the overall mass. In marine applications, increased allowable topside loads and the reduced draft may permit easier movement out of dry docks and through shallow shipping channels **(1)**.

Several investigations have been made about the effect of steel fiber addition on the behavior of the reinforced concrete beams (2-5).

Nevertheless, in spite of the advantages that have been reported in this area, much more research is still needed. This is especially so because the variability in the characteristics of the lightweight aggregate used. Added to that is the diversity of the types of fibers and the various choices that are available within each type.

Hence, the research focus of this study is the effects of different steel fiber geometry (shape), volume fraction and replacing natural sand with lightweight sand on the structural behavior of high performance lightweight aggregate concrete beams reinforced with ordinary steel reinforcement.

2. Experimental Program

2.1 Materials

Ordinary Portland cement (Type I) was used for all concrete mixtures. The chemical composition of the cement is given in Table (1). Condensed silica fume (CSF) was used from Holicm materials. The amount retained on a 45-µm sieve was 0.77%. Detailed chemical composition is given in Table 1. The lightweight aggregate used in this study was pumice produced manually in accordance to the requirements of ASTM C 330. The particle specific gravity of the dry aggregate was 2.53 and the loose bulk density was 571 kg/m^3. The nominal particle size ranges from 4.75 to 12.5 mm with an irregular shape. The aggregate had water absorption of 1.8%, 2.8% and 4.9%, at 15 minutes, 1 h and 24 h respectively. Natural sand with a fineness modulus of 3.0 and a specific gravity of 2.63 was used. A high range water reducing admixture known commercially as Sikament-FFN was used. Two types of steel fibers were used, crimped and hooked fibers. Their properties are listed in Table (2). Deformed steel bars were used for longitudinal reinforcements and stirrups in the beams, the properties are shown in Table 3.

Tab. 1: Chemical Composition of Cementitious Material

Chemical Composition (%)	**OPC**	**CSF**
Silicon dioxide (SiO_2)	20.38	91.8
Aluminum oxide (Al_2O_3)	4.69	1.6
Ferric Oxide (Fe_2O_3)	2.85	2.35
Calcium oxide (CaO)	62.76	0.37
Magnesium oxide (MgO)	2.44	1.65
Sodium oxide (Na_2O)	0.24	---
Potassium oxide (K_2O)	0.64	---
Sulfur trioxide (SO_3)	2.5	0.53
Loss on ignition	3.3	4.9

Tab. 2: Properties of Steel Fibres

Parameter	**Crimped**	**Hooked**
Length (mm)	30	30
Diameter (mm)	0.6	0.6
Density (g/cm^3)	7.85	7.85
Elasticity Modulus (GPa)	210	210
Tensile Strength (MPa)	>2000	>2000
Aspect ratio	50	50

Tab. 3: Properties of Steel Reinforcement

Parameter	**Longitudinal Reinforcement**	**Longitudinal /Stirrups Reinforcement**
Diameter (mm)	12	10
Yield Strength (MPa)	500.7	510
Tensile Strength (MPa)	765.8	755.92
Modulus of Elasticity (GPa)	200	200
Elongation (%)	20.13	18.76

2.2 Mix Proportions

The weight of material per m^3 shown in Table 4 was selected after many trial mixes and it was used throughout this study in casting beams. The volume fraction of steel fibers in concrete was (0.5, 1.0 and 1.25) % for the both types. All mixes had 3% of super-plasticizer and 10% silica fume by weigh of cement.

2.3 Mixing

Before mixing, the pumice is pre-soaked for (15 minutes) in water and used after removal of excess surface water by drier (10-15 minutes). Every Mixture has been made with the same mixing procedure:

Rotary drum was dampened prior to the mixing. Coarse lightweight aggregate was added first to the drum (surface dry). Fine normal weight aggregate was introduced to the drum (dry). Fine lightweight aggregate was then introduced to the drum (if any) (dry) mixture was homogenized for 1 minute. After that, cement and silica fume was added to the rotary drum, and then two thirds of the water was also added to the rotary drum. Finally super-plasticizer and one third of water were added to the rotary drum. Mixture was mixed for 6 minutes.

When fibers were used, for each type of fiber, three different contents (0.5%, 0.75% and 1.25%) by volume were used. The matrix materials were mixed first and then fibers were progressively added into the mix by hand, the addition was during a mix period of about 1.5 minute and the whole mixture was mixed for about 1.0 minute after adding the last piece of fiber.

Tab. 4: Selected Mix Design Proportions

Concrete ingredients	
Cement content (kg/m^3)	572.3
Normal weight fine aggregate (sand) (kg/m^3)	763
Lightweight coarse aggregate (Pumice)(kg/m^3)	481.8
Water (kg/m^3) (mixing water with S.P.)	247.4
Super-plasticizer (S.P.)	3%*
Silica Fume (kg/m^3)	57.23
W/C	0.432
Water-Cementitious Material Ratio	0.393
Slump(mm)	(50 -100)±5

*of cement weight

2.4 Curing

After casting, the molds were covered with polyethylene sheets for about 24hrs to ensure a humid air around the specimens and then de-molded for curing. All the specimens were cured by the same method which consisted of covering the specimens with burlap and spraying them with water three times daily, the specimens were cured continuously for 28 days and kept in open air until the beginning of the tests.

2.5 Experimental test

A number of standard test specimens of different sizes were cast for investigating the various parameters. 100mm cubes were used for studying the compressive strength. Split tensile strength test was conducted on (100x200) mm cylindrical molds. Prisms of (100x100x400) mm were used for flexural strength test.

Compressive strength and splitting tensile strength tests were carried out in a testing machine of 2000-kN capacity according to BS 1881 part 116 for the former and ASTM C 496 for the latter. While flexural strength conducted on prisms using a testing machine of 200-kN capacity in accordance to ASTM C78.

2.6 Load Carrying Capacity Test

The beams were rectangular in cross section, 150 mm in width, 250 mm in overall depth and 2000 mm long. The fiber content and the other variables are listed in Table 5.

The reinforcement details of the beams are shown in Fig. (1). All beams were provided with longitudinal reinforcement both in tension and compression. Transverse reinforcement consists of Φ10mm bars, bent into closed stirrups used with a clear concrete cover of 20 mm on all sides throughout the test program. All beams were provided with the same spacing of stirrups in the shear zone sufficient enough to ensure flexural failure prior to any shearing stress. No stirrups were used in the flexural zone (central 400mm).

Tab. 5: Test Beam Variables

Beam Label	**Fiber**		**Fine Aggregate**	
	Type	**Volume Fraction (%)**	**Natural Sand (%)**	**Pumice Sand (%)**
B-LAC-1		0	100	0
B-LAC-2	Crimped	0.5	100	0
B-LAC-3	Crimped	0.75	100	0
B-LAC-4	Crimped	1.25	100	0
B-LAC-5	Hooked	0.5	100	0
B-LAC-6	Hooked	0.75	100	0
B-LAC-7	Hooked	1.25	100	0
B-LAC-8		0	0.75	0.25
B-LAC-9	Crimped	0.75	0.75	0.25

B-LAC-10	Hooked	0.75	0.75	0.25

The test beams were simply supported and subjected to two, symmetrically placed, point loads. The distance between the two loadings points was kept at 600 mm and each shear span was 600 mm. Details of the test set-up are shown in Fig. (2). The beams were suitably instrumented for measuring deflections at the mid-span by means of a dial gauge [(Hommel-Germany) brand with accuracy of 0.01mm], rotation of the beam at each end by using mechanical inclinometers, locating discs (demec points) at gauge length of (200) mm measured by a punch bar, a mechanical extensometer [Model 35-2884 (CT-171m), ELE International] to measure concrete strains at specific locations and levels at mid-span, under the unit loads, between the unit loads and the supports as illustrated in Fig. (3).

Initially, the beams were exercised by applying a load of about 5 kN and then releasing the load to overcome any slack between the specimen, the loading and support systems. All the instruments were then initialized. The beam was loaded in increments of 9 kN until failure.

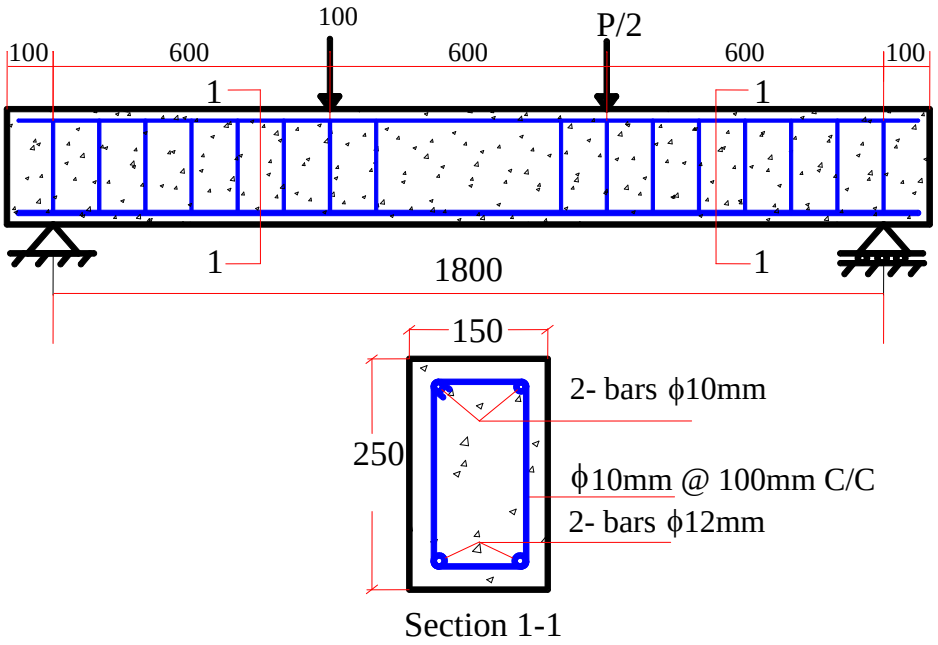

Fig. 1: Beam Reinforcement Details

The load was applied by a hand operated hydraulic jacking system and all deformation readings were taken at preset load intervals until final collapse. All the macro-cracks observed were also marked and recorded during the testing for each loading stage.

Fig. 2: Test Set-up Details

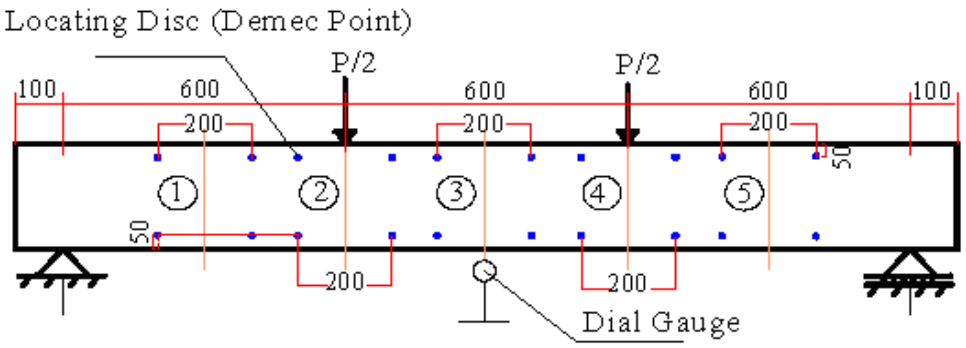

Fig. 3: Arrangement of Locating Disis

3. Results and Discussion

3.1 Mechanical Properties of control specimens

The control specimen of high performance lightweight aggregate concrete (HPLWAC) reinforced with fibers were tested at 28 and 120 days and the results of mechanical properties of specimens are presented in Table (6).

3.1.1 Compressive Strength

The variation of compressive strength of HPLWAC specimens with fiber volume fraction for different steel types of fibers (crimped and hooked) is shown in Table (6). It can be

seen that the compressive strength of concrete specimens not influenced significantly by the addition of steel fibers. This may be due to their material properties, under compression loading, when micro-cracking occurs as a result of transverse tension forces, steel fibers cause crack-closing forces and this leads to an increase of compressive strength. While, porosity increases slightly when steel fibers are mixed with the fresh concrete. This effect decreases the compressive strength of steel fiber reinforced concrete. Both effects in combination have the tendency to a little increase in compressive strength [(6)]. Since the steel fibers are high strength materials, they contribute to the strengthening component of concrete in compression by delaying the unstable growth of micro-cracks, resulting in strength increase and strains at peak load [(7)].

The table also shows that the average percentage of increase is 3.44, 5.5 and 8.8 for specimens containing 0.5%, 0.75% and 1.25% fibers. This difference in compressive strength increase is due to that, in case of the hooked end fibers, the interaction of the matrix and the fibers at the hooked ends is capable of carrying the most applied load while in the case of crimped fibers, the total length has been corrugated which means multiple interaction points carrying most the applied loads and more better mechanical anchorage [(8)]. While in LAC-8, LAC-9 and LAC-10 specimens where 25% of the normal sand has been replaced with pumice sand, there is a decrease in the compressive strength of the concrete with or without fibers by (9, 5 and 2) % respectively due to sand replacement which in turn reduces the strength of the matrix.

3.1.2 Splitting Tensile Strength

In general, it can be seen from Table (6) that the splitting tensile strength improves by the addition of steel fibers. The average percentage of increase in splitting tensile strength of the fiber HPLW reinforced concrete is 40, 45 and 70 for specimens containing 0.5%, 0.75% and 1.25% crimped and hooked fibers respectively. This may be attributed to high tensile strength of the fibers and the well bond of steel fibers to the matrix.

While in LAC-9 and LAC-10 the percentage increase in the splitting tensile strength of the fiber reinforced concrete is (37.3 and 35) respectively for the specimens containing 0.75% crimped and hooked fibers.

3.1.3 Modulus of Rupture

The effect of volume fraction of steel fibers on modulus of rupture (ultimate flexural strength) of HPLWAC specimens is shown in Table (6).

The percentage increase in the modulus of rupture of the fiber reinforced concrete is 11.9, 27.5 and 54.1 for specimens containing 0.5%, 0.75% and 1.25% crimped fibers respectively, while for the same ratio of fiber content for the specimens incorporated hooked fibers is 6.9, 16.7 and 39.1 respectively. There is a higher increase in modulus of rupture where the concrete specimens incorporated crimped steel fibers due to multiple interaction points carrying most the applied loads and more better mechanical anchorage because of the corrugated shape along the length of the fibers. But in case of the hooked end fibers, the interaction of the matrix and the fibers are only at the hooked end which is capable of carrying the most applied load [(9)].

While in LAC-9 and LAC-10 specimens the percentage increase in the modulus of rupture of the fiber reinforced concrete is (6.8 and 7.4) for the specimens containing 0.75% crimped and hooked fibers respectively. The percentages are lower than companion

specimens containing the same fiber volume fraction and type with normal sand. This may be attributed to the sand replacement which reduces the strength of the matrix and this has a role in decreasing the modulus of rupture. It can be seen also that the ratio of flexural strength to compressive strength of control specimen is (0.12) while this ratio increases to (0.13, 0.14, and 0.16) for the specimens containing crimped steel fibers (0.5%, 0.75% and 1.25%) by volume respectively with an average slight increase of 2.3% more than the reference concrete. In case of the specimens with hooked steel fiber content (0.5%, 0.75% and 1.25%) by volume the ratio is (0.12, 0.13 and 0.15) respectively with an average increase of 1.3% more than the unreinforced specimen. This ratio for LAC-9 and LAC-10 specimens is unchanged in comparison to LAC-3 and LAC-6 specimens with the same fiber content and type.

3.2 Behavior of the FRLWAC Beams in Flexure

Generally, all beams showed typical structural behavior in flexure. No horizontal cracks were observed at the level of the reinforcement, which indicated that there were no occurrences of bond failure. Vertical flexural cracks were observed in the constant-moment region and final failure occurred due to the damage of the tension concrete with a significant amount of ultimate deflection. Since all beams were under-reinforced (nearly two and half folds the minimum reinforcement), yielding of the tensile reinforcement occurred before crushing of the concrete cover in the pure bending zone.

Tab. 6: Compressive Strength, Splitting Tensile Strength and Modulus of Rupture of Control and HPFRLWA Concrete

Mix ID	Fiber		Sand Content (%)		Compressive Strength		Splitting Tensile Strength		Modulus of Rupture	
	Type	(%) by Volume	Normal	Pumice	MPa					
					Days		Days		Days	
					28	120	28	120	28	120
LAC-1		0	100	0	46.9	52	3.29	3.65	5.6	6.07
LAC-2	C	0.5	100	0	49.45	54.07	4.88	5.14	6.51	6.79
LAC-3		0.75	100	0	50.07	54.83	4.97	5.35	6.5	7.74
LAC-4		1.25	100	0	52.78	57.53	5.7	6.26	8.02	9.35
LAC-5	H	0.5	100	0	49.06	53.87	4.6	5.06	5.25	6.49
LAC-6		0.75	100	0	50.48	54.87	4.8	5.23	6.36	7.08
LAC-7		1.25	100	0	50.71	55.57	5.65	6.17	7.25	8.44
LAC-8		0	75	25	43.03	47.33	3.18	3.52	5.07	5.82
LAC-9	C	0.75	75	25	44.97	49.37	4.56	5.01	5.5	6.48
LAC-10	H	0.75	75	25	46.71	51	4.49	4.93	5.23	6.52

C = Crimped, H = Hooked, HPFRLWA=High Performance Fiber Reinforced Lightweight Aggregate

3.2.1 Load-deflection Relationship

In general, the shape of load deflection curve of the beams reinforced with steel fibers from the both types crimped and hooked is tri-broken curvilinear segments. The first ends at the point of first crack, the second with a smaller slope than that of the first which ends at the point of yielding of the tensile steel reinforcement, then the last with a smaller slope than that for the second which ends at the point of failure. It can be seen from the load-deflection curves in Fig (4) that for the beams containing 0.5% crimped or hooked by volume, the shape is similar to that of the beam without fiber with a little increase in the slope of the curvilinear segments of the curve with a higher cracking, yielding and failure loads in comparison to the reference beam. While for the beams containing 0.75% crimped or hooked by volume, the shape is similar to that of the beam with 0.5% by volume of fiber with a little increase in the slope of the curvilinear segments of the curve with the same cracking and higher yielding and failure loads than that of the beams containing 0.5% steel fibers. For the beams reinforced with 1.25% crimped or hooked by volume, the shape is similar to that of the beam with 0.75% by volume of fiber with a little increase in the slope of the curvilinear segments of the curve with the same cracking and higher yielding and failure loads than that of the beams containing 0.75% steel fibers .

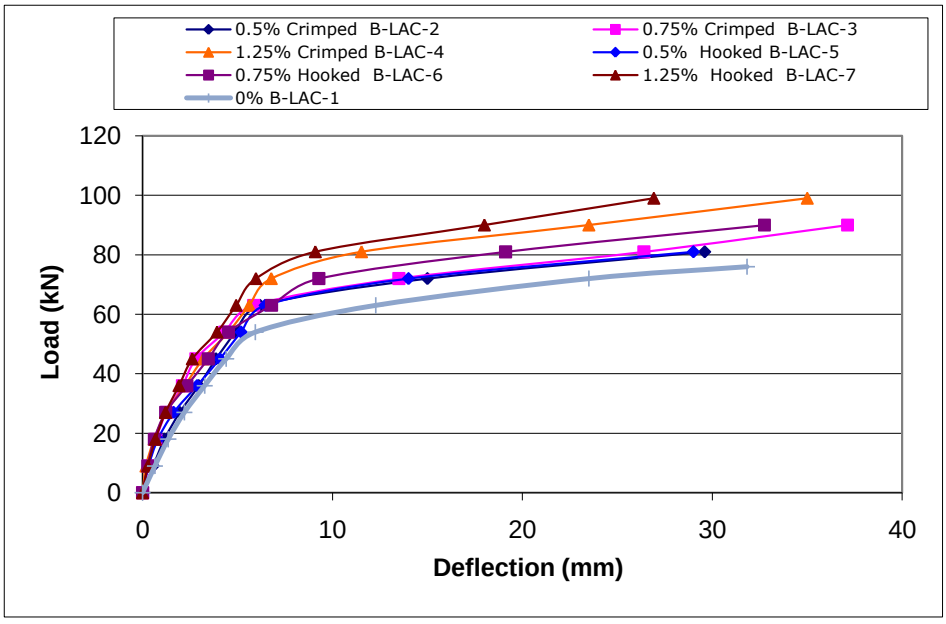

Fig. 4: Typical Load-deflection Curves for HPFRLWAC Beams

3.2.2 First Crack and Ultimate Loads Capacity

Based on the results in table (7), it is obvious that the load carrying capacity of the beams reinforced with fiber increases with the increase in fiber volume fraction, the increase was (6.5, 18.4 and 30.2) % for the fiber content of (0.5, 0.75 and 1.25) % by volume respectively and for both types of fibers crimped and hooked when compared to the reference beam. On the other hand, for the beams (B-LAC-9 and B-LAC-10) that contain 25% pumice sand, the increase was 6.5% which is in turn less than that of the companion

beams with the same volume fraction of fiber from both types due to normal sand replacement with pumice sand which affects the strength of the matrix as previously mentioned. The first cracking load for all the beams containing steel fibers also increases by 33% in comparison to the control beam (without fiber).

3.2.3 Ductility

It can be noted from Table (7) that the percentage increase in curvature ductility of the FRLWA concrete beams as a result of inclusion of steel fiber of crimped type (0.5%, 0.75% and 1.25%) by volume was (10.7, 41.6 and 53.6) respectively, while for the same fiber content but hooked type was (5.6, 39.9 and 51) respectively. It is obvious from the results that the curvature ductility directly related to the fiber volume concentration as shown in Fig (4-19). A slight difference in the ductility between the beams containing crimped steel fibers and the other beams reinforced with hooked steel fibers was noticed as a result of the geometry of the fibers used which in turn affects the bond to the matrix (i.e. better bond in the case of crimped fibers). In the beam B-LAC-8 due to the reduction in concrete strength, as a result of replacing 25% of the normal sand with pumice sand, was the reason behind the reduction in the ductility of the beam by 20.3%. The same above justification is applicable to the beams B-LAC-9 and 10 as the sand replacement reduced the strength of the concrete which in turn yielded lower ductility ratios.

In general, the results are within the limits that are reported by Ashour [10] that the members with displacement ductility in the range of 3 to 5 have adequate ductility and can be considered for structural members subjected to large displacements.

Beam ID	Fiber		First Cracking		Ultimate		Curvature at Yield Φ_y (1/mm)	Curvature at Ultimate Φ_u (1/mm)	Curvature Ductility Ratio
	Type	(%) by volume	Load (P_{cr}) (kN)	Deflection (mm)	Load (P_u) (kN)	Deflection (mm)			
B-LAC-1[a]		0	27	2.20	76	31.83	1.735E-05	9.288E-05	5.35
B-LAC-2[a]	C	0.5	36	2.96	81	29.60	1.718E-05	1.018E-04	5.92
B-LAC-3[a]		0.75	36	2.10	90	37.12	1.714E-05	1.299E-04	7.58
B-LAC-4[a]		1.25	36	2.23	99	35.0	1.710E-05	1.407E-04	8.22
B-LAC-5[a]	H	0.5	36	2.87	81	29.0	1.710E-05	1.071E-04	6.26
B-LAC-6[a]		0.75	36	2.33	90	32.75	1.707E-05	1.278E-04	7.49
B-LAC-7[a]		1.25	36	1.92	99	26.92	1.693E-05	1.368E-04	8.08
B-LAC-8[b]		0	27	1.76	72	20.53	1.763E-05	7.470E-05	4.24
B-LAC-9[b]	C	0.75	36	2.05	81	27.31	1.729E-05	1.113E-04	6.44
B-LAC-10[b]	H	0.75	36	2.06	81	26.90	1.719E-05	1.047E-04	6.09

a, 100% Natural Sand, Sand-lightweight Concrete b, (25% Pumice Sand, 75% Natural Sand), 75% Sand-lightweight Concrete , C=crimped, H=hooked

Tab. 7: Load and Deflection at First Crack and Ultimate of Control and HPFRLWAC Beams with Curvature Ductility Ratio

3.2.4 Moment Rotation Relationship

The moment-end rotation relationship of the beams is shown in Fig. (5).In general, the shape of moment-end rotation curve of the beams reinforced with steel fibers from both types crimped and hooked is tri-broken curvilinear segments. The first ends at the point of first crack, the second with a smaller slope than that of the first ends at the point of yielding of the tensile steel reinforcement, then the last with a smaller slope than that for the second which ends at the point of failure. It can be seen also from Fig (5) that the load-deflection curves that for the beams containing 0.5% crimped or hooked by volume, the shape is similar to that of the beam without fiber with a little increase in the slope of the curvilinear segments of the curve with a higher cracking, yielding and failure loads in comparison to the reference beam. While for the beams containing 0.75% crimped or hooked by volume, the shape is similar to that of the beam with 0.5% by volume of fiber with a little increase in the slope of the curvilinear segments of the curve with the same cracking and higher yielding and failure loads than that of the beams containing 0.5% steel fibers. On the other hand, for the beams reinforced with 1.25% crimped or hooked by volume the shape is similar to that of the beam with 0.75% by volume of fiber with a little increase in the slope of the curvilinear segments of the curve with the same cracking and higher yielding and failure loads than that of the beams containing 0.75% steel fibers.

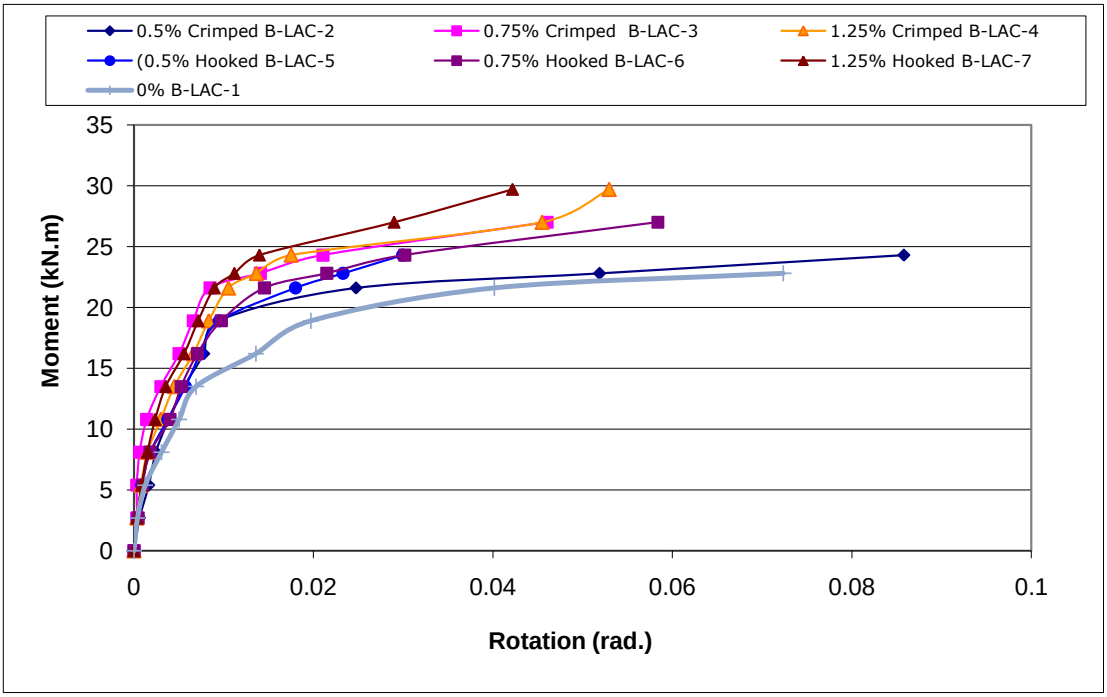

Fig. 5: Typical Moment-End rotation Curves for HPFRLWAC Beams

3.2.5 Cracking Patterns and Modes of Failure

In general, it can be seen that the beams exhibited similar cracking patterns, a flexural mode of failure characterized by flexural cracks, and deformation was distributed fairly equally among the cracks before yielding of the reinforcing steel, and then it was concentrated at two or three cracks after yielding. Cracks in the fiber reinforced concrete (FRC) beams developed quite close to an adjacent crack. Using of steel fibers reduced from one side the crack width and spacing and resulted in a greater number of cracks on the other side, compared to the control reinforced concrete beam as shown in Fig (6 & 7)

Tension stiffening in the case of FRC is that the concrete is able to carry tension at the cracks in addition to the tension between the cracks which effectively stiffens the member response (increases member rigidity). Due to this phenomenon, FRC can exhibit significant amounts of post-cracking tensile strength at a crack, depending on the type and content of fibers used in addition to a reduced crack spacing and control of cracks width.

In all the beams with or without fiber reinforcement, the first crack occurred in the central test zone (600mm). In specimen B-LAC-1, the first crack was near to the right point load, while in B-LAC-8 specimens, directly under the right point load. In case of the beams containing crimped fibers, the first crack was between the mid-span and the right point load in specimen B-LAC-2, B-LAC-3 and B- LAC-4. For the other beams, B-LAC-5, B-LAC-6 and B-LAC-7 were reinforced with hooked fibers the first crack was at mid-span, near to the left point load for the other two latter beams. On other hand the first crack location, for both beams B-LAC-9 and B-LAC-10 was near to the left point load.

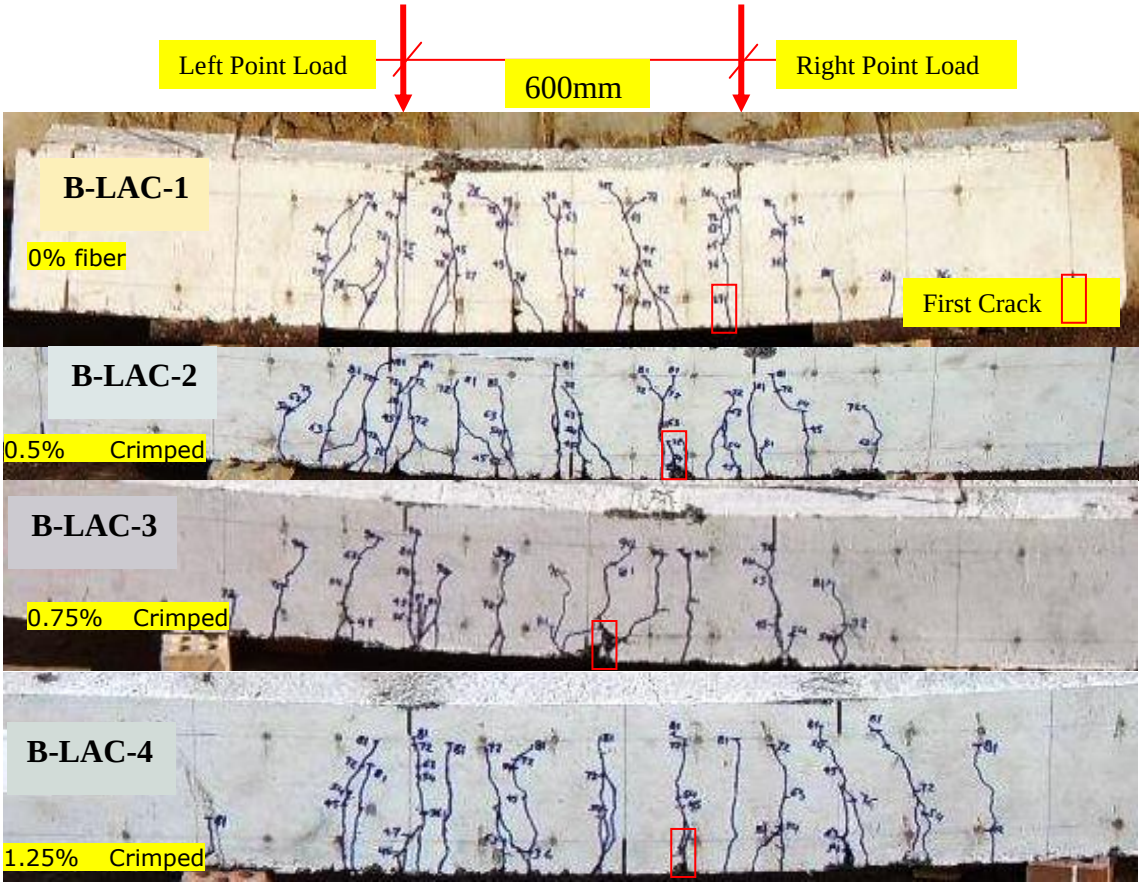

Fig. 6: Crack Patterns of HPLWC Beams after Failure with/without Fibers

3.2.6 Toughness and Toughness Indexes

The most important reasons for adding discontinuous steel fibers to a concrete matrix are to improve the post-cracking response of the concrete (i.e., to improve its energy absorption capacity and apparent ductility) and to provide crack resistance and crack control. For fiber-reinforced concrete (FRC), the concept of flexural toughness (which is a measure of the energy absorption capacity of a material and is used to characterize the material's ability to resist fracture when subjected to static strains or dynamic impact loads) is often used to characterize these important improvements.

There are a number of different standards for measuring toughness of fiber-reinforced concrete such as ASTM C1018 and Japanese Concrete Institute JCI SF-4 (method of tests for flexural strength and flexural toughness of fiber reinforced concrete. In JCI SF-4 method, the area under the load deflection curve up to a deflection of (span/150) is obtained and results obtained from this test method yield an absolute toughness value. A flexural toughness factor is calculated which has a unit of stress. This factor can be considered as the post crack residual strength of the material when loaded to a deflection of (span/150). In the present work, the toughness indexes suggested in ASTM C1018 are used because of its wide acceptance and use for design and construction. It can be noted from table (8), that the toughness indexes of the beam B-LAC-2 incorporating 0.5% by volume crimped fiber has the highest I_5 index among all the other beams which is 12.5, while the highest I_{10} index is 28.4 for the beam B-LAC-5 with 0.5% hooked fiber by volume.

On the other hand (I_{20}) for B-LAC-2 could not be calculated as the deflection at failure for the beams is less than the first crack deflection multiplied by (10.5) factor. In this case, the index of B-LAC-6 has a greater value of 54.9. Accordingly the residual strength factor $R_{5,10}$ for the beam B-LAC-5 was the highest (323.2), while the residual strength factor ($R_{10,20}$) was the greater for B-LAC-6 with a value of 311.2.The difference between the index values is due to the type of the fiber used in the beams. It is obvious that only one volume concentration of fibers 0.5% from both types yielded the largest values of (I_5) and (I_{10}) in addition to $R_{5,10}$. But for I_{20} and $R_{10,20}$, the beam containing 0.75% hooked fiber has the largest values. The same type of results has been confirmed by Altun *et al* [5], the indexes related to 0.4% by volume content of steel fibers were higher than the relative indexes of 0.8% by volume content from the same fiber.

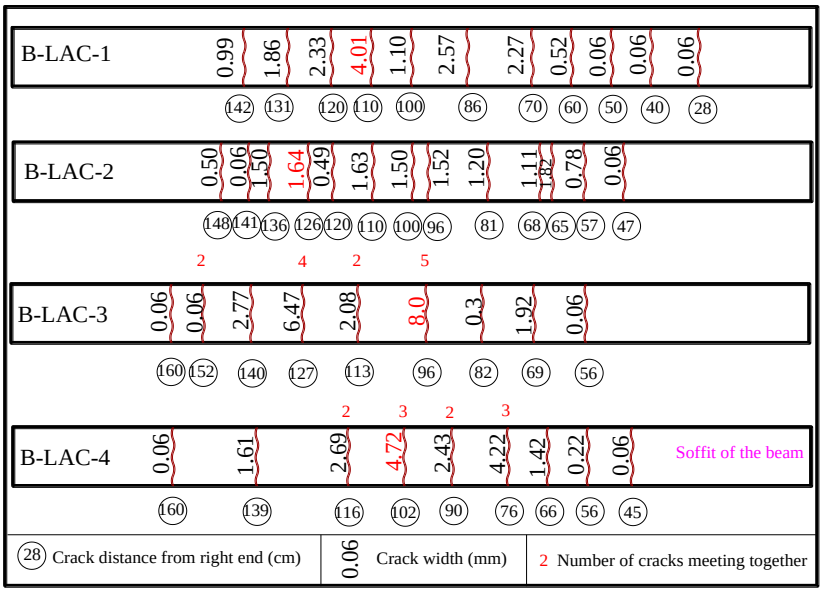

Fig. 7: Cracks at the soffit of HPLWC Beams after Failure with/without Fibers

Tab. 8: Toughness Index and Residual Strength Factor of Control and HPFRLWAC

Beam ID	Fiber		Toughness Index			Residual Strength Factor	
	Type	(%) by Volume	I_5	I_{10}	I_{20}	$R_{5,10}$	$R_{10,20}$
B-LAC-1		0	7.20	17.40	41.20	204.6	237.5
B-LAC-2	Crimped	0.5	12.5	28.30	----	316	----
B-LAC-3		0.75	8.30	19.20	43.40	217.5	242.3
B-LAC-4		1.25	9.20	22.10	51.60	259.3	294.4
B-LAC-5	Hooked	0.5	12.2	28.40	-----	323.3	----
B-LAC-6		0.75	9.80	23.80	54.90	279.7	311.2
B-LAC-7		1.25	7.90	19.50	46.0	233	264.9
B-LAC-8		0	5.40	13.30	31.40	157.5	181.2
B-LAC-9	Crimped	0.75	7.30	17.80	40.70	210	229.3
B-LAC-10	Hooked	0.75	7.50	18.50	38.10	220.3	196.3

---- Not applicable

3.2.7 Strain Distribution

The addition of fibers to the concrete mixtures increased the strain of the sample corresponds to the peak stress (ultimate compressive strain). The strain capacity and deformation capability of the concrete matrix are increased considerably with the inclusion of steel fibers (SF) to the mixtures due to confinement effect induced by the distributed steel fibers in a concrete matrix. Increasing peak strain is the highest for the fiber having higher volume fraction. The ascending portions of the load–strain curves are affected by the addition of SF. Since the tests were carried out in a load controlled manner, the descending portion of the load-strain curves could not be obtained as this portion of the curve only could be obtained with a testing machine with the capability of performing deformation controlled loading.

The strain over the depth of the tested LW concrete beams has been measured on the surface, where demec points were fixed, by using an ELE mechanical strain gauge and the values at mid-span section are plotted for different loads. A typical strain distribution diagram at mid-span section is presented in Fig (9). While the strain distribution diagrams at the sections 0.3m from the left and right supports were disregard due to the limited influence on the performance of the beam specimen. On other hand due to a strong similarity among the strain distribution diagrams at the mid-span and under the left and right unit loads, the diagram at the mid-span is regarded as the typical strain distribution diagram for all the beam specimens.

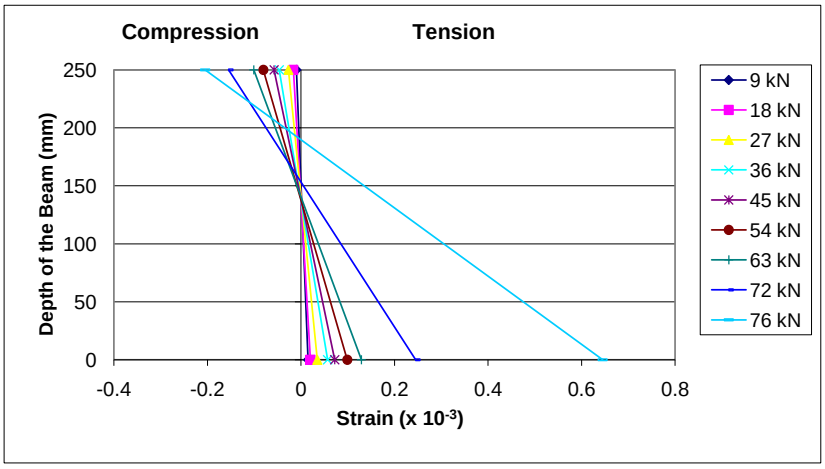

Fig. 9: Change in Strain in the Cross Section during Loading for Specimen B-LAC-1 (Mid-Span)

Fig (10) shows the load-strain curves of HPFRLWAC beams, the compressive strains at a level of 50mm from the top of the section of the beam at mid-span with the applied load till the failure, it can be noted that the strain increases directly with increase in the fiber content of the beams till reaching the peak value. The peak value of strain for fiber content of (0.5, 0.75 and 1.25) % crimped type was (3.65, 4.21 and 4.6) x 10^{-3} respectively as a result of strain hardening effect due to the fiber inclusion. While the peak strain for the beams including the same volume concentration of hooked fibers was (3.55, 4.1 and 4.58) x 10^{-3} respectively the slight difference in the peak value is due to the fiber geometry. Generally, the strain of LWC in the range of ($3.3x10^{-3}$ – $4.6x10^{-3}$) has been reported by Zhang and Gjorv **(11)**.

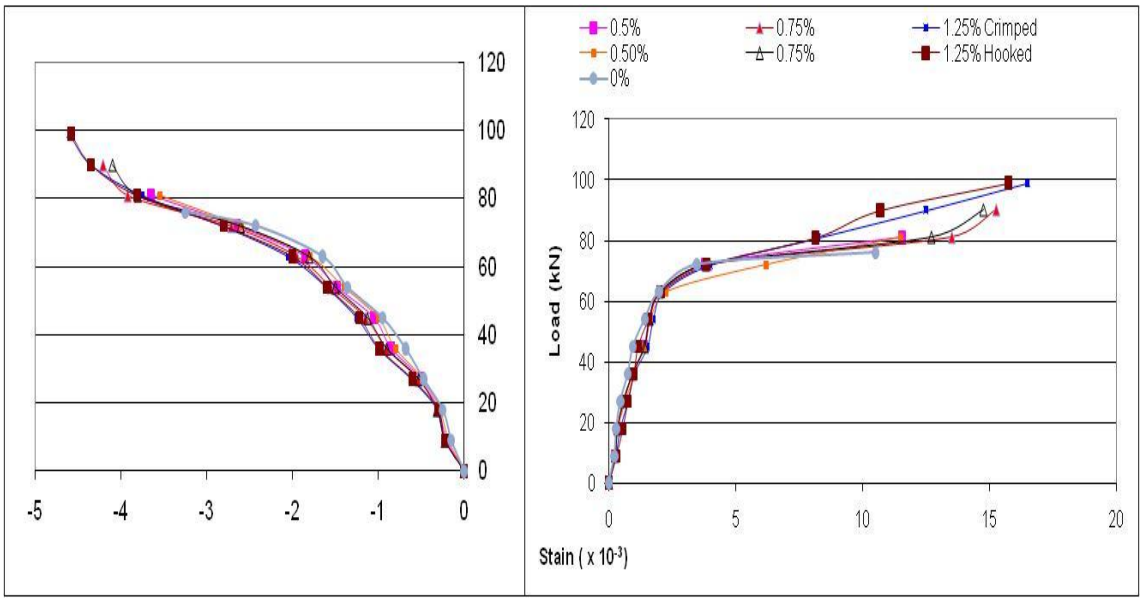

Fig. 10: Load-strain Curves for HPFRLWAC Beams

It can be seen also from Fig (10) that the load-strain curves of HPFRLWAC beams the tensile strains at a level of 50mm from the bottom of the section of the beam at mid-span with the applied load till the failure. It can be noted that the strain increases directly with increase in the fiber content of the beams till reaching the peak value. The peak value of strain for fiber content of (0.5, 0.75 and 1.25) % crimped type was (11.56, 15.25 and 16.5) x 10^{-3} respectively as a result of strain softening effect due to the fiber inclusion. While the peak strain for the beams including the same volume concentration of hooked fibers was (11.52, 14.75 and 15.75) x 10^{-3} respectively the slight difference in the peak value is due to the fiber geometry.

3.3 Flexural Analysis of Beams Containing Bars and Fibers

The flexural strength analysis is based on the conventional compatibility and equilibrium conditions used for normal reinforced concrete and the contribution of the steel fibers in the tension zone are also recognized. Since inclusion of steel fibers is greatly increase the tensile capacity of the concrete as indicated in the previous sections. This analysis is based on the compression stress block incorporated in ACI Code 318-08. The actual and assumed stress and strain distributions at failure are shown in Fig (11). The height (g) of the elastic un-cracked zone of concrete is very small compared to the neutral axis depth (c) and it is therefore assumed that the tensile contribution of the steel fibers is represented by a rectangular stress block over the whole of the tension zone of the beam [(2)].

The flexural strength of FRC composites material may be described as the sum of matrix strength and fiber strength as follows [(4)]:

$$\sigma_{c\,t} = \sigma_{mt}\rho_m + \sigma_f\,\rho_f \qquad \text{.....(1)}$$

where:

σ_{ct} =flexural strength of FRC composite; σ_{mt} = flexural strength of matrix; σ_f = strength of fibers; ρ_m = volume ratio of matrix(=1- ρ_f); and ρ_f = fiber volume ratio.

Since the orientation, length and bonding characteristics of fibers will influence the strength of FRC, these parameters must be incorporated into (1).

$\sigma_{ct} = \sigma_{mt}\,\rho_m + F_o\,F_l\,F_b\,\sigma_f\,\rho_f$ …….. (2)

where:

F_o ,F_l ,F_b = orientation factor, length efficiency factor and bond efficiency factor of fibers respectively.

By neglecting the contribution of the concrete matrix at ultimate state due to tensile cracking of the concrete matrix, the first term of the right-hand side of (2) vanishes. The fiber strength σ_f may be derived from the bonding characteristics of fibers as follows:

$\sigma_f = 2\tau(l_f/d_f)$ Ref. (12) …….. (3)

in which τ = bond strength of fiber. The ultimate strength (σ_t) of FRC is now summarized as:

$\sigma_t = 2F_oF_lF_b\rho_f\tau(l_f/d_f)$ …….. (4)

$F_o = 0.41$ [5]

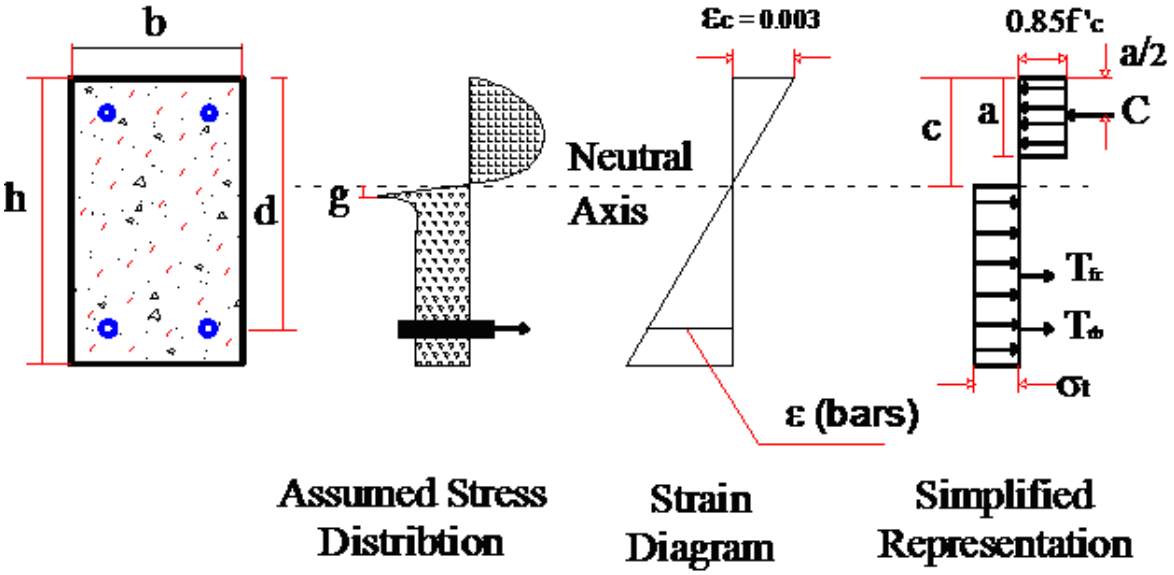

Fig. 11: Design Assumption for Analysis of Singly Reinforced Concrete Beams Containing Steel Fibers (Swamy) [2]

F_l = 0.5, since the fiber length (l_f = 30mm) is less than the fiber critical length (l_c = 289mm) [13]

F_b = 1.2 for crimped and hooked steel fibers [2]

τ = 2.3 and 4.15 MPa, for normal and high strength concrete respectively [14], the final expression of (σ_t) after substituting all above factors and (τ) will be as follows:

For high strength concrete

$$\sigma_t = 0.02\rho_f(l_f/d_f) \qquad \text{..... (5a)}$$

For normal strength concrete

$$\sigma_t = 0.011\rho_f(l_f/d_f) \qquad \text{..... (5b)}$$

The deduced equation of nominal moment (M_n) of FRC beams with conventional steel bars is:

$$M_n = A_s f_y\left(d - \frac{a}{2}\right) + \frac{\sigma_t b(h-c)(h+c-a)}{2} \qquad \text{..... (6)}$$

For normal strength lightweight concrete:

$$c = \frac{A_s f_y + \sigma_t bh}{0.90 f'_c \beta_1 b + \sigma_t b} \qquad \text{..... (7a)}$$

For high strength lightweight concrete:

$$c = \frac{A_s f_y + \sigma_t bh}{0.85 f'_c \beta_1 b + \sigma_t b} \qquad \text{.....(7b)}$$

Where:

A_s= area of tension reinforcement, (mm^2)

f_y= yield strength of reinforcing bar, (MPa)

f'_c = concrete compressive strength, (MPa)

d=distance from extreme compression fiber to centroid of tension reinforcement (effective depth), (mm)

c = neutral axis depth, (mm)

a = depth of a rectangular stress block, (mm)

β_1=factor defined in section 10.2.7.3 ACI Code (318-08)

σ_t = tensile stress in fibrous concrete, (MPa)

b = width of beam, (mm), h = total depth of beam, (mm)

The theoretical and corresponding experimental load carrying capacity of the beams that were tested in this investigation is indicated in table (9). It can be noted that the proposed model equation underestimate the load carrying of the beams B-LAC-3, B-LAC-4, B-LAC-6 and B-LAC-7 containing 0.75% and 1.25% of steel fibers from both types crimped and hooked respectively. While for the other beams the predictions of load carrying capacity were closer to the experimental results. It can be also seen that for the beams without fibers, this models yield the same prediction closer to the current experimental value for B-LAC-1 and an overestimated value for B-LAC-8. For the beams that contain steel fibers, the predictions according to the Lim *(et al)*'s[3] model is more conservative than the proposed model, while the other model (ACI-544)[15] yielded more conservative predictions than the Lim (*et al)*'s model.

It can be observed that the ultimate tensile strength of fiber reinforced concrete increases with the increase of the volume fractions and reduces the tensile stress in embedded tension steel reinforced bars in beams, therefore the neglect of fiber contribution yields serious errors in estimating the flexural capacity of the beams, the same results were noticed by other researchers [4,14].

Tab. 9: Comparison of the Experimental Load-carrying Capacity with their Corresponding Theoretically Predicted Values (kN)

Beam ID	**Fiber**		**Experimental P_{max} (1)**	**Theoretical Model**					
				Proposed		**ACI-544**		**Lim**	
	Type	**(%) by Volume**		**P_{max} (2)**	**(2) / (1)**	**P_{max} (3)**	**(3) / (1)**	**P_{max} (4)**	**(4) / (1)**
B-LAC-1[a]		0	76	77.10	1.01	76.88	1.01	77.10	1.01
B-LAC-2[a]	C	0.5	81	83.82	1.03	79.97	0.98	81.87	1.00
B-LAC-3[a]		0.75	90	87.12	0.96	81.48	0.90	84.22	0.93
B-LAC-4[a]		1.25	99	93.80	0.94	84.58	0.85	89.00	0.89
B-LAC-5[a]	H	0.5	81	83.77	1.03	79.92	0.98	81.82	1.01
B-LAC-6[a]		0.75	90	87.12	0.96	81.48	0.90	84.22	0.93
B-LAC-7[a]		1.25	99	93.57	0.94	84.40	0.85	88.82	0.89
B-LAC-8[b]		0	72	76.49	1.06	76.49	1.06	76.73	1.06
B-LAC-9[b]	C	0.75	81	81.95	1.01	80.95	0.99	83.69	1.03
B-LAC-10[b]	H	0.75	81	82.12	1.01	81.11	1.00	83.86	1.03

a, 100% Natural Sand, Sand-lightweight Concrete b, (25% Pumice Sand, 75% Natural Sand), 75% Sand-lightweight Concrete, C=crimped, H=hooked

4. Conclusions

From the results of this investigation, the following conclusions can be drawn:

1. The failure load of specimen beams increased by (6.5, 18.4 and 30.2) % as the volume fraction of fiber (0.5, 0.75 and 1.25) % increases respectively and for the both types of fibers (crimped and hooked). While the average increase of cracking load for all the beams was 33% in comparison to the specimen without fiber.
2. The results show that the curvature ductility of high performance LWC beams increases with the increase in volume fraction of steel fibers (crimped and hooked). The average increase was (8.2, 40.8, 52.3) % as v_f = 0.5, 0.75, 1.25% respectively.
3. The shape of the moment-end rotation curve follows the same general pattern of the load-deflection curve of the corresponding beam, in which the rotation increases linearly with increase in moment until yielding of steel occurred.
4. Generally, all beams showed similar structural behavior in flexure. No horizontal cracks were observed at the level of the reinforcement, which indicated that there were no occurrences of bond failure. Vertical flexural cracks were observed in the constant-moment region and final failure occurred due to damage of the tension concrete with a significant amount of ultimate deflection.
5. Toughness of all the fiber reinforced LWC beams is considerably enhanced relative to unreinforced specimen, the value of toughness index (I_5, I_{10}) was the highest for v_f = 0.5%, while I_{20} index was the highest for v_f = 0.75% (among all the other FRC beams).
6. The addition of fibers increases the strain corresponding to the peak compressive stress (ultimate compressive strain). The strain capacity and deformation capability of the concrete matrix are increased considerably with the increase in volume fraction of fibers.
7. For the beams that contain steel fibers, the predictions to calculate the failure loads according to the proposed theoretical model were closest to the current experimental results.

5. References

[1] Satish Chandra & Leif Berntsson, "Lightweight Aggregate Concrete", 1st Edition, Noyes Publications/William Andrew Publishing, 2002.

[2] Swamy R. N, Sa'ad A. Al-Ta'an, " Deformation and Ultimate Strength in Flexure of Reinforced Concrete beams Made with Steel Fiber Concrete", ACI Journal Proceedings, Vol. 78, No. 5, 1981, pp (395-405).

[3] Lim T. Y, Paramasivan P, Lee S. L, "Shear and Moment Capacity of Reinforced Steel Fiber Concrete Beams", Magazine of Concrete Research, Vol. (39), No. (140), 1987, pp. 148-160.

[4] Buyung Hwan Oh, "Flexural Analysis of Reinforced Concrete Beams Containing Steel Fibers", ASCE, Journal of Structural Engineering, Vol. 118, No. 10, 1992, pp (2821-2836).

[5] Altun, Fatih; Haktanir, Tefaruk; Ari, Kamura, “Effects of Steel Fiber Addition on Mechanical Properties of Concrete and RC Beams", Construction and Building Materials Magazine, www.highbeam.com, 2007.

[6] Lars Kutzing and Gert Konig, " Design Principals for Steel Fiber Reinforced Concrete – A fracture Mechanics Approach", Leipzig Annual Civil Engineering Report (LACER), Vol. 4, 1999, pp (175-183).

[7] P. Balaguru & M. G. Dipsia, "Properties of Fiber Reinforced High Strength Semi-lightweight Concrete", ACI Materials Journal, Vol. (90), No. (5), 1999, pp. (399-405).

[8] Brend Weiler and Christian Grosse, "Pullout Behavior of Fibers in Steel Fiber Reinforced Concrete", Stuttgart University, Annual Journal on Research and Testing Materials, Vol. 7, 1996, pp. (116-127).

[9] R. V. Balendran, F. P. Zhou, A. Nadeem and A. Y. T. Leung," Influence of Steel Fibers on Strength and Ductility of Normal and Lightweight High Strength Concrete", Building and Environment Journal, Vol. 37, No. (12), 2002, pp. (1361-1367).

[10] Ashour, S. A., "Effect of Compressive Strength and Tensile Reinforcement Ratio on Flexural Behavior of High-strength Concrete Beams, Journal of Engineering Structures, Vol. (22), No. (5), 2000, pp (413-423).

[11] Min Hong Zhang and Odd E. Gjvorv, "Mechanical Properties of High-strength Lightweight Concrete", ACI Materials Journal, Vol. (88), No. (3), 1991, pp. (240-247).

[12] Callister, William D, “Materials Science and Engineering: An Introduction”, John Wiley & Sons, Inc. New York NY, 1994, p (522).

[13] Lim T. Y, P. Paramasivan and S.L. Lee,” Analytical Model for Tensile Behavior of Steel Fiber Concrete”, ACI Materials Journal, Vol. 84, No. 4 , 1987, pp (286-298)

[14] Dancygier A. N., Z. Savir, "Flexural Behavior of HSFRC with Low Reinforcement Ratios", the Journal of Engineering Structures, Vol. (28), No. (11), 2006, pp. (1503-1512)

[15] ACI Committee 544, "Design Considerations for Steel Fiber Reinforced Concrete", ACI 544.4R-88 (Reapproved 1999)